



A Mononuclear Copper Electrocatalyst both Water Reduction and Oxidation

| | |
|-------------------------------|--|
| Journal: | <i>RSC Advances</i> |
| Manuscript ID: | RA-ART-07-2014-007211.R1 |
| Article Type: | Paper |
| Date Submitted by the Author: | 10-Sep-2014 |
| Complete List of Authors: | Zhan, Shuzhong; College of Chemistry & Chemical Engineering, South China University of Technology, Fu, Ling-Zhi; South China University of Technology, Fang, Ting; South China University of Technology, Zhou, Ling-Ling; South China University of Technology, |
| | |

ARTICLE

A Mononuclear Copper Electrocatalyst both Water Reduction and Oxidation

Cite this: DOI: 10.1039/x0xx00000x

Ling-Zhi Fu, Ting Fang, Ling-Ling Zhou and Shu-Zhong Zhan*

Received 00th January 2012,
Accepted 00th January 2012

DOI: 10.1039/x0xx00000x

www.rsc.org/

The oxidation and reduction of water is a key challenge in the production of chemical fuels from electricity. Although several catalysts have been developed for these reactions, substantial challenges remain towards the ultimate goal of an efficient, inexpensive and robust electrocatalyst. Until now, there is as yet no report on both water oxidation and reduction by identical catalyst. Reported here is a soluble copper-based catalyst, $\text{Na}_2[\text{Cu}(\text{opba})]$ **1** (opba: o-phenylenebis(oxamato) for water oxidation and reduction. Water oxidation occurs at an overpotential of 636 mV vs SHE to give O_2 with a turnover frequency (TOF) of $\sim 1.13 \text{ s}^{-1}$. Electrochemical studies also indicate that **1** is a soluble molecular species, that this is the most rapid homogeneous water-reduction catalyst, with a TOF of 1331.7 (pH 7.0) moles of hydrogen per mole of catalyst per hour in a pH 7.0 buffer at an overpotential of 788 mV vs SHE. Sustained water reduction catalysis occurs at glassy carbon (GC) to give H_2 over a 36 h electrolysis period with 96.5% Faradaic yield and no observable decomposition of the catalyst.

Introduction

Splitting water to molecular oxygen is a high energy density method for storing solar energy in the form of chemical fuels.¹⁻⁴ This endergonic electrochemical conversion stores 1.23 V and consists of the four electrons, four proton oxidation of water to oxygen and the reduction of the produced protons to hydrogen. One of the key challenges to water splitting is the development of efficient catalysts for the water. These considerations have led to the development of molecular catalysts employing more abundant metals, and several complexes that contain nickel,⁵ cobalt⁶ and molybdenum⁷ have been developed as electrocatalysts for the reduction of water to form H_2 . Another notable progress has been made in homogeneous water oxidation catalysis with transition metal complexes, including manganese,⁸⁻¹¹ cobalt,¹²⁻¹⁴ copper^{15,16} and iron.¹⁷⁻²⁴ Despite much progress in water oxidation and reduction catalysis, major improvements in several areas, including lowering overpotentials, increasing catalyst durability, and using earthabundant elements, are needed before efficient electrocatalytic water splitting can be realized.

In designing a model featuring both water oxidation and reduction functionality, we sought a synthetic cofactor with following inspired properties: (1) The metal center coordination geometry is planar; (2) Mild redox couple closer to the H_2/H^+ couple and $\text{O}_2/\text{H}_2\text{O}$ couple, in the range -0.75 to -1.45 V and 0.40 to 1.23 V versus SHE, respectively; (3) Chemical inertness, so that reactions would be localized at the metal centers. Reported here is a water-soluble copper electrocatalyst, $\text{Na}_2[\text{Cu}(\text{opba})]$ **1** (opba: o-phenylenebis(oxamato) that can catalyze both water oxidation and reduction.

Results and discussion

The synthesis of $\text{Na}_2[\text{Cu}(\text{opba})]$ **1** (opba: o-phenylenebis(oxamato) was carried out according to the literature.²⁵ **1** is very soluble in water and insoluble in organic solvents, such as methanol and ethanol. The UV-vis spectrum was recorded in aqueous solution, with main features at 257, 313 and 327 nm (Fig. S1). And the UV-vis spectra of **1** in buffered aqueous solutions in pH 4.4 to 12.6 exhibit similar peaks to those in water. When pH = 11.8, the absorption band at 257 nm disappeared, suggesting that complex **1**

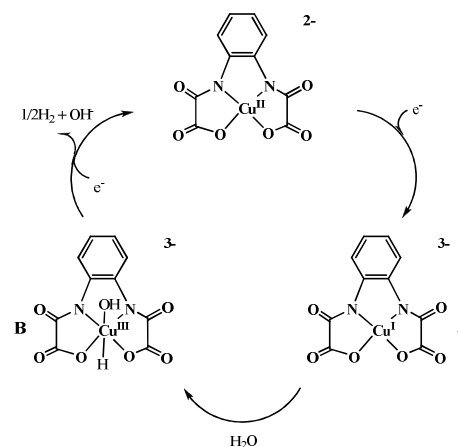
decomposes to a new component under these conditions (Fig. S2). Therefore, we will explore its electrochemical properties in pH 4.4 to 10.8.

The cyclic voltammogram (CV) of an aqueous solution of **1** (Fig. S3) shows a reversible wave at $E_{1/2} = -0.05$ V (all potentials vs Ag/AgCl) and an irreversible wave at 0.96 V, which are assigned to a metal-based $\text{Cu}^{\text{II}}/\text{Cu}^{\text{I}}$ redox event and a $\text{Cu}^{\text{III}}/\text{Cu}^{\text{II}}$ couple, respectively. Sweeping toward the anode shows one irreversible redox wave at 0.96 V, which can be assigned to $\text{Cu}^{\text{III}}/\text{Cu}^{\text{II}}$ couple. We further explored the electrochemical behavior of **1** in buffered aqueous solution where $\text{pH} = 3.6\text{--}11.4$ which is the range associated with catalytic water reduction and oxidation. In pH 7.0 phosphate buffer, a reversible $\text{Cu}^{\text{II}}/\text{Cu}^{\text{I}}$ wave at -0.21 V was observed for **1** (Fig. 1). The $\text{Cu}^{\text{III}}/\text{Cu}^{\text{II}}$ couple displays a pH-dependent redox potential change, with a slope of -67 mV/pH in the range from pH 3.6 to 7.0 (Fig. S4), suggesting a proton-coupled electron transfer process. CVs were also recorded at different scan rates in order to obtain kinetic information of this complex. The current response of the redox event at -0.21 V shows a linear dependence on the square root of the scan rate (Fig. S5), which is an indicative of a diffusion-controlled process, with the electrochemically active species freely diffusing in the solution.

Correspondingly, sweeping toward the cathode reveals one irreversible redox wave at -1.20 V, which is assigned to a metal-based $\text{Cu}^{\text{I}}/\text{Cu}^{\text{0}}$ couple (Fig. 1). The current response of the redox events at -1.20 V also varies linearly on the square root of the scan rate (pH 7.0), which is an indicative of a diffusion-controlled process (Fig. S6). Sweeping toward the anode shows one irreversible redox wave at 0.89 V (pH 7.0), which can be assigned to a metal-based $\text{Cu}^{\text{III}}/\text{Cu}^{\text{II}}$ (Fig. 1). A number of control experiments were carried out to verify that complex **1** is responsible for the catalysis. In particular, the free ligand, CuSO_4 , and a mixture of the free ligand and CuSO_4 were each measured under identical conditions. As can be seen in Figs. S7-Fig. S9, the catalytic competency achieved with **1** is not matched by neither the free ligand alone, CuSO_4 , or the mixture of the free ligand and CuSO_4 , as might arise from dissociation of the ligand; nor can it be accomplished with the ligand bound to a redox-inactive metal. Thus, a combination of the redox-active copper and the ligand is essential for catalytic activity.

First, we explored the catalytic water reduction by complex **1**. As shown in Fig. 2-(a), **1** shows a pH-dependent peak between -1.06

and -2.0 V versus Ag/AgCl, these peaks are responsible for catalytic water reduction. The onset of this catalytic current is clearly influenced by the solution pH, the applied potential declines with decreasing pH, evidencing the involvement of a proton in the initial stage of electrochemical catalysis. Meanwhile, there is an obvious potential gap between the onset of the catalytic current and the $\text{Cu}^{\text{I}}/\text{Cu}^{\text{0}}$ redox event. From these observations we propose that reduction of $\text{Cu}^{\text{I}}/\text{Cu}^{\text{0}}$ is a proton-coupled redox process. On the basis of literature precedent²⁶ and above analyses, we propose the catalytic cycle depicted in Scheme 1 for the generation of hydrogen from water mediated by **1**. One-electron reduction of $\text{Na}_2[\text{Cu}(\text{opba})]$ **1** gives a putative $[\text{Cu}(\text{opba})]^{3-}$ species (**A**). Addition of water yields the $\text{Cu}^{\text{III}}\text{-H}$ species (**B**), a high reactive intermediate. Further reduction of the $\text{Cu}^{\text{III}}\text{-H}$ species affords $1/2\text{H}_2$, releases one OH^- anion and regenerates the starting complex **1**. Further mechanistic studies are under investigation.



Scheme 1 The possible catalytic mechanism for water reduction by complex **1**

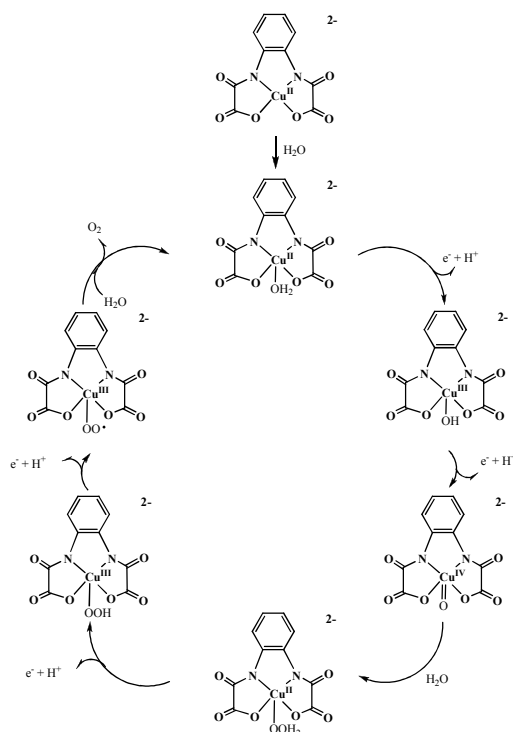
Fig. 2-(b) shows the total charge of bulk electrolysis of complex **1** at pH 7.0. When an applied potential was -1.45 V vs Ag/AgCl, the maximum charge was only 144 mC during 2 min of electrolysis in absence of complex **1** (Fig. S10). Under the same conditions, the charge reached 1.20 C with addition of copper complex **1**, accompanying a large amount of gas bubble appeared (Fig. S11), which was confirmed to be H_2 by GC analysis. The evolved H_2 was analyzed by gas chromatography, Fig. 3-(a), which gave ~ 6.4 mL of H_2 over an electrolysis period of 1 h with a Faradaic efficiency of 96.5% for H_2 (Fig. 3-(b)). TOF for electrocatalytic hydrogen production by complex **1** is 1331.7 moles of hydrogen per mole of

catalyst per hour in a pH 7.0 buffer at an overpotential of 788 mV vs SHE (Fig. 2-(c)).

To the best of our knowledge, this value is significantly higher than some reported molecular catalysts for electrochemical hydrogen production from neutral water, including a dinickel complex that exhibits a turnover number of 100 moles of H₂ per mole of catalyst with a turnover frequency of 160 moles of H₂ per mole of catalyst per hour at an overpotential of 820 mV²⁷ and a cobalt complex displaying a turnover number of 5 moles of H₂ per mole of catalyst with a turnover number of 0.4 moles of H₂ per mole of catalyst per hour at an overpotential of 390 mV,²⁸ and can be compared to a molybdenum-oxo complex that shows a maximum of 1,600 moles of H₂ per mole of catalyst per hour at an overpotential of 642 mV [7].

We further explored the catalytic water oxidation by complex **1**, a much more attractive field. CVs were conducted in buffers at different pH values. At more positive potentials, one irreversible oxidation wave appear at 0.89 V vs Ag/AgCl in 0.25 M buffer (pH 7.5), corresponding to Cu^{III}/Cu^{II} (Fig. 4-(a)), with a greatly enhanced underlying current compared to the background. Fig. 4-(b) exhibits a systematic in *i*_{cat} with increasing pH from 7.5 to 11.4. Cyclic voltammograms of background in the absence of complex **1** exhibit no catalytic current at the potential of the couple of Cu^{III}/Cu^{II}, suggesting that water oxidation to O₂ occurs with complex **1**.²⁹ The current enhancement for the wave at E_{p,a} = 0.89 V is consistent with catalytic water oxidation, with catalytic onset shift to more negative potentials (from 1.30 V to 0.78 V). When the pH was 10.1, the peak at 0.89 V disappeared, indicating a new component was formed. When the pH reached 10.8, one new irreversible oxidation wave appeared at E_{p,a} = 1.18 V, which can be assigned to Cu^{IV}/Cu^{III} couple. The current enhancement for the wave at E_{p,a} = 1.18 V is consistent with catalytic water oxidation. When the pH reached 11.4, another new irreversible oxidation wave appeared at E_{p,a} = 1.63 V, and the peak at 1.18 V got weak, indicating complex **1** was decomposing. The current enhancement for the wave at E_{p,a} = 0.89 V ([Cu^{III}(opba)]/[Cu^{II}(opba)]²⁻) is consistent with catalytic water oxidation at pHs 7-8.5, with catalytic onset shift to more negative potentials (from 1.30 V to 0.80 V). And the current enhancement for the wave at E_{p,a} = 1.18 V ([Cu^{IV}(opba)]/[Cu^{III}(opba)]⁻) is also consistent with catalytic water oxidation at pH>10.1, with catalytic onset shift to more negative potentials (from 1.30 V to 0.95 V). Based on the above observations, both couples [Cu^{III}(opba)]⁻

and [Cu^{IV}(opba)]/[Cu^{III}(opba)]⁻ are devoted to water oxidation. Analysis of the anodic scans of the redox couples at 0.90 V (pH 8.7) and 1.20 V (pH 10.8) as a function of scan rates (Fig. S12 and Fig. S13) both show a linear relation, consistent with adsorption of the molecules on the electrode surface. Such distinctive potentials prompted possible usage of copper complex **1** as an electrocatalyst for water oxidation reaction. Based on these observations, a mechanism for water oxidation is proposed in Scheme 2. In this mechanism, the product of the second oxidation would be the formally Cu^{IV} species, a high-oxidation Cu-oxo intermediate as sites for O-O coupling and water oxidation, as found in other complexes.³⁰⁻³³



Scheme 2 The possible catalytic mechanism for water oxidation by complex **1**

Further evidence for the electro-catalytic activity of complex **1** was obtained by bulk electrolysis of an aqueous solution of complex **1** (2.8 μM) with phosphate buffer (0.25 M) at variable potential using an ITO electrode in a double-compartment cell. A series of applied potentials were chosen, corresponding to the electro-catalytic potentials observed in cyclic voltammograms. As shown in Fig. 4-(c) (pH 10.8), the amount of charge used in 2 min increases with increasing the applied potential until a saturation value of 0.41 C is reached at 1.35 V vs Ag/AgCl, accompanying the formation of a

large amount of gas bubble (Fig. S14), can be attributed to the catalytic generation of O₂ from water. Then, the charge significantly decreased when the applied potential was set to more positive. This saturation behavior occurs because the potential drop between the working and auxiliary electrodes exceeds the maximum output voltage of the potentiostat at high current densities, and is not an inherent property of the catalyst. Compared to that at pH 10.8, at pH 8.7, a very small saturation value of 0.016 C is reached at 1.55 V vs Ag/AgCl (Fig. 4-(d)).

Water oxidation occurs at an overpotential of 626 mV vs SHE, based on the half-peak potential for CVs at pH 10.8 and 100 mV/s, and the reversible potential for $4e^- + O_2 + 4H^+ = 2H_2O$ of 0.52 V at this pH. This overpotential is comparable to the reported homogeneous water-oxidation catalysts (600–900 mV).³⁴⁻³⁷

Evolution of O₂ as a product was investigated by controlled potential electrolysis at 1.23 V vs Ag/AgCl on a large surface area ITO (1.32 cm²) electrode with 2.8 μM complex **1** in 0.25 M phosphate buffer (pH 10.8). The background for oxygen formation at the applied potential in the absence of catalyst is small (Fig. S15). After a 5 h electrolysis period, pH decreased by 1.5 units (from 10.6 to 9.1), consistent with consumption of OH⁻ by water oxidation, $4OH^- + 4e^- \rightarrow 2O_2 + 2H_2O$. The evolved O₂ was analyzed by gas chromatography, Fig. 5-(a), which gave ~96 μmol of O₂ over an electrolysis period of 5 h with a Faradaic efficiency of 95.8% for O₂ (Fig. 5-(b)).

This study stated clearly that **1** is capable of catalyzing the oxidation of water to O₂. According to eq. (1) [16], n_p is the number of electrons transferred in the noncatalytic wave, n_c is mol of electrons required to generate a mol of O₂ and v is the scan rate. From the slope of the plot of i_{cat}/i_d versus $v^{-1/2}$ (Fig. S12 and Fig. S13), we calculated k_{cat} , which is usually referred as turnover frequency (TOF) of the catalyst in the literature, for the catalyst reaching a maximum of 0.14 s⁻¹ ($E_{p,a} = 0.83$ V, and Eq. 2), and 1.13 s⁻¹ ($E_{p,a} = 10.8$ V, and Eq. 3), respectively, indicating that $[Cu^{IV}(opba)]/[Cu^{III}(opba)]^-$ plays a larger role than $[Cu^{III}(opba)]^-/[Cu^{II}(opba)]^{2-}$ for water oxidation. This value (1.13 s⁻¹) is higher than some reported molecular water oxidation catalysts,³⁸⁻⁴⁰ yet lower than the recently reported copper based ones.^{15,41}

$$\frac{i_c}{i_p} = 0.359 \frac{n_c}{n_p^{3/2}} \sqrt{k_{cat}/v} \quad (1)$$

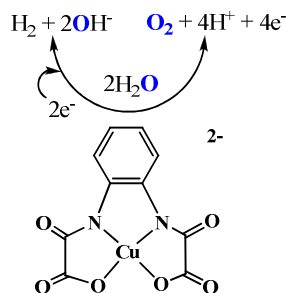
The durability of catalyst **1** for water reduction and oxidation were also tested in an extended CPE experiment performed in a 0.25 M buffer at pH 7.0 and pH 10.8, respectively. As depicted in Fig. S16, the catalyst affords a robust and essentially linear charge build-up over time, with no substantial loss in activity over the course of 36 h for water reduction. As observed in Fig. S17, the catalyst affords a robust and essentially linear charge build-up over time, with no substantial loss in activity over the course of 10 h. After a 10 h electrolysis period, the charge build-up slightly increased due the decrease in pH, consistent with consumption of H⁺ by water oxidation, $2H_2O - 4e^- \rightarrow O_2 + 4H^+$. The original catalytic function was recovered and could be repeated at least 10 times when the solution pH was adjusted back to the original 10.8.

To prove complex **1** as a homogeneous electrocatalyst, we obtained dependence of the catalytic current on complex **1** concentration. As shown in Fig. S18, the observation of the catalytic current being dependent of the complex concentration could indicate a homogeneous catalyst. And several pieces of evidence also suggest that this mononuclear copper complex is a homogeneous catalyst: 1) There is no evidence for a heterogeneous electrocatalytic deposit. For example, the electrode was rinsed with water and electrolysis at -1.45 V vs Ag/AgCl was run for an additional 2 min in a 0.25 M phosphate buffer at pH 7.0 with no catalyst present in solution. During this period, ca. 144 mC of charge was passed, a similar magnitude as is observed for electrolysis conducted with freshly polished electrodes. 2) No discoloration of the electrodes was observed during cyclic voltammetry or bulk electrolysis.

Experimental

Cyclic voltammograms were obtained on a CHI-660E electrochemical analyzer under oxygen-free conditions using a three-electrode cell in which a glassy carbon electrode GC was the working electrode, a saturated Ag/AgCl electrode was the reference electrode, and platinum wire was the auxiliary electrode. Controlled-potential electrolysis (CPE) in aqueous media was conducted using an air-tight glass double compartment cell separated by a glass frit. The working compartment was fitted with a glassy carbon plate or an ITO plate and an Ag/AgCl reference electrode. The auxiliary compartment was fitted with a Pt gauze electrode. The working compartment was filled with 50 mL of 0.25 M phosphate buffer solution at different pH values, while the auxiliary compartment was

filled with 35 mL phosphate buffer solution. Dinuclear copper complex **1** was then added and cyclic voltammograms were recorded. After electrolysis, a 0.5 mL aliquot of the headspace was removed and replaced with 0.5 mL of CH₄. A sample of the headspace was injected into the gas chromatograph (GC). GC experiments were carried out with an Agilent Technologies 7890A gas. UV-Vis spectra were recorded on a U-3900H spectrophotometer.



Conclusions

In summary, a water soluble mononuclear copper complex **1**, which is very easy to be obtained, can catalyze both water oxidation and reduction. Electrochemical studies show that **1** is the first soluble molecular copper species, that is among the most rapid homogeneous water-reduction catalysts, with a TOF of 1331.7 (pH 7.0) moles of hydrogen per mole of catalyst per hour at an overpotential of 788 mV vs SHE. Water oxidation occurs at an overpotential of 636 mV vs SHE to give O₂ with a turnover frequency (TOF) of ~1.13 s⁻¹ (pH 10.8). This discovery has established a new chemical paradigm for creating water oxidation and reduction catalysts that is highly active and robust in purely aqueous media.

Acknowledgements

This work was supported by the National Science Foundation of China (No. 20971045, 21271073), and the Student Research Program (SRP) of South China University of Technology.

Notes and references

College of Chemistry and Chemical Engineering, South China University of

Electronic Supplementary Information (ESI) available: [details of any supplementary information available should be included here]. See DOI: 10.1039/b000000x/

1 D. G. Nocera, *Inorg. Chem.*, 2009, **48**, 10001–10017.

2 N. S. Lewis and D. G. Nocera, *Proc. Natl. Acad. Sci. U.S.A.*, 2006, **103**, 15729–15735.

3 D. Abbott, *Proc. IEEE.*, 2010, **98**, 42–66.

4 T. R. Cook, D. K. Dogutan, S. Y. Reece, Y. Surendranath, T. S. Teets and D. G. Nocera, *Chem. Rev.*, 2010, **110**, 6474–6502.

5 B. J. Fisher and R. Eisenberg, *J. Am. Chem. Soc.*, 1980, **102**, 7361–7363.

6 W. M. Singh, T. Baine, S. Kudo, S. Tian, X. A. N. Ma, H. Zhou, N. J. DeYonker, T. C. Pham, J. C. Bollinger, D. L. Baker, B. Yan, C. E. Webster and X. Zhao, *Angew. Chem. Int. Ed.*, 2012, **51**, 5941–5944.

7 H. I. Karunadasa, C. J. Chang and J. R. Long, *Nature* 2010, **464**, 1329–1333.

8 J. Limburg, J. S. Vrettos, L. M. Liable-Sands, A. L. Rheingold, R. H. Crabtree and G. H. Brudvig, *Science* 1999, **283**, 1524–1527.

9 G. C. Dismukes, R. Brimblecombe, G. A. N. Felton, R. S. Prydun, J. E. Sheats, L. Spiccia and G. F. Swiegers, *Acc. Chem. Res.*, 2009, **42**, 1935–1943.

10 Y. Gao, R. H. Crabtree and G. W. Brudvig, *Inorg. Chem.*, 2012, **51**, 4043–4050.

11 M. Wiechen, H. Berends and P. Kurz, *Dalton Trans.*, 2012, **41**, 21–31.

12 Q. Yin, J. M. Tan, C. Besson, Y. V. Geletii, D. G. Musaev, A. E. Kuznetsov, Z. Luo, K. I. Hardcastle and C. L. Hill, *Science* 2010, **328**, 342–345.

13 D. K. Dogutan, R. McGuire and D. G. Nocera, *J. Am. Chem. Soc.*, 2011, **133**, 9178–9180.

14 D. J. Wasylenko, C. Ganesamoorthy, J. Borau-Garcia and C. P. Berlinguette, *Chem. Commun.*, 2011, **47**, 4249–4251.

15 S. M. Barnett, K. I. Goldberg and J. M. Mayer, *Nat. Chem.*, 2012, **4**, 498–502.

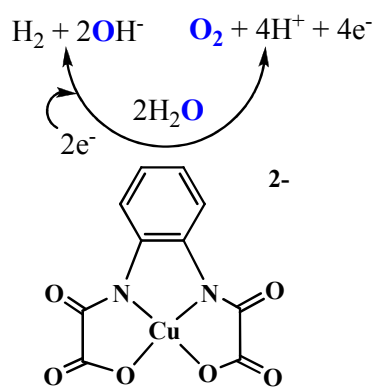
16 T. Zhang, C. Wang, S. Liu, J. Wang and W. Lin, *J. Am. Chem. Soc.*, 2014, **136**, 273–281.

17 W. C. Ellis, N. D. McDaniel, S. Bernhard and T. J. Collins, *J. Am. Chem. Soc.*, 2010, **132**, 10990–10991.

18 J. Lloret-Fillol, Z. Codol, I. Garcia-Bosch, L. Gmez, J. J. Pla and M. Costas, *Nat. Chem.*, 2011, **3**, 807–813.

19 I. Garcia-Bosch, Z. Codol, I. Prat, X. Ribas, J. Lloret-Fillol and M. Costas, *Chem. Eur. J.*, 2012, **18**, 13269–13273.

- [20] M. Z. Ertem, L. Gagliardi and C. J. Cramer, *Chem. Sci.* **2012**, *3*, 1293–1299.
- 21 R. Sarma, A. M. Angeles-Boza, D. W. Brinkley and J. P. Roth, *J. Am. Chem. Soc.*, 2012, **134**, 15371–15386.
- 22 D. Hong, Y. Yamada, T. Nagatomi, Y. Takai and S. Fukuzumi, *J. Am. Chem. Soc.*, 2012, **134**, 19572–19575.
- 23 G. Chen, L. Chen, S. Ng, W. Man and T. Lau, *Angew. Chem. Int. Ed.*, 2013, **52**, 1789–1791.
- 24 M. K. Coggins, M. Zhang, A. K. Vannucci, C. J. Dares and T. J. Meyer, *J. Am. Chem. Soc.*, 2014, **136**, 5531–5534.
- 25 H. O. Stumpf, Y. Pei, O. Kahn, J. Metten and J. P. Renardt, *J. Am. Chem. Soc.*, 1993, **115**, 6738–6745.
- 26 S. Mandal, S. Shikano, Y. Yamada, Y.-M. Lee, W. Nam, A. Llobet and S. Fukuzumi, *J. Am. Chem. Soc.*, 2013, **135**, 15294–15297.
- 27 J. P. Collin, A. Jouaiti and J. P. Sauvage, *Inorg. Chem.*, 1988, **27**, 1986–1990.
- 28 P. V. Bernhardt and L. A. Jones, *Inorg. Chem.*, 1999, **38**, 5086–5090.
- 29 P. Kang, E. Bobyr, J. Dustman, K. O. Hodgson, B. Hedman, E. I. Solomon and T. D. P. Stack, *Inorg. Chem.*, 2010, **49**, 11030–11038.
- 30 M.-T. Zhang, Z. Chen, P. Kang and T. J. Meyer, *J. Am. Chem. Soc.*, 2013, **135**, 2048–2051.
- 31 Z. F. Chen, J. J. Concepcion, X. Q. Hu, W. T. Yang, P. G. Hoertz and T. J. Meyer, *Proc. Natl. Acad. Sci. U.S.A.*, 2010, **107**, 7225–7229.
- 32 D. J. Wasylenko, C. Ganesamoorthy, M. A. Henderson, B. D. Koivisto, H. D. Osthoff and C. P. Berlinguette, *J. Am. Chem. Soc.*, 2010, **132**, 16094–16106.
- 33 J. F. Hull, D. Balcells, J. D. Blakemore, C. D. Incarvito, O. Eisenstein, G. W. Brudvig and R. H. Crabtree, *J. Am. Chem. Soc.*, 2009, **131**, 8730–8731.
- 34 J. J. Concepcion, J. W. Jurss, M. K. Brennaman, P. G. Hoertz, A. O. T. Patrocinio, N. Y. M. Iha, J. L. Templeton and T. J. Meyer, *Acc. Chem. Res.*, 2009, **42**, 1954–1965.
- 35 R. Lalrempuia, N. D. McDaniel, H. Muller-Bunz, S. Bernhard and M. Albrecht, *Angew. Chem. Int. Ed.*, 2010, **49**, 9765–9768.
- 36 N. D. Schley, J. D. Blakemore, N. K. Subbaiyan, C. D. Incarvito, F. D'Souza, R. H. Crabtree and G. W. Brudvig, *J. Am. Chem. Soc.*, 2011, **133**, 10473–10481.
- 37 J. G. McAlpin, T. A. Stich, C. A. Ohlin, Y. Surendranath, D. G. Nocera, W. H. Casey and R. D. Britt, *J. Am. Chem. Soc.*, 2011, **133**, 15444–15452.
- 38 J. F. Hull, D. Balcells, J. D. Blakemore, C. D. Incarvito, O. Eisenstein, G. W. Brudvig and R. H. Crabtree, *J. Am. Chem. Soc.*, 2009, **131**, 8730–8731.
- 39 W. C. Ellis, N. D. McDaniel, S. Bernhard and T. J. Collins, *J. Am. Chem. Soc.*, 2010, **132**, 10990–10991.
- 40 J. Concepcion, J. Jurss, P. Hoertz and T. Meyer, *Angew. Chem. Int. Ed.*, 2009, **48**, 9473–9476.
- 41 M. Zhang, Z. Chen, P. Kang and T. J. Meyer, *J. Am. Chem. Soc.*, 2013, **135**, 2048–2051.



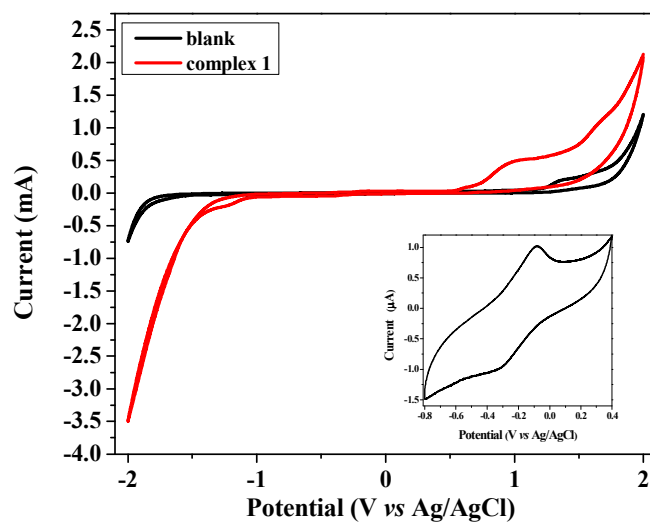
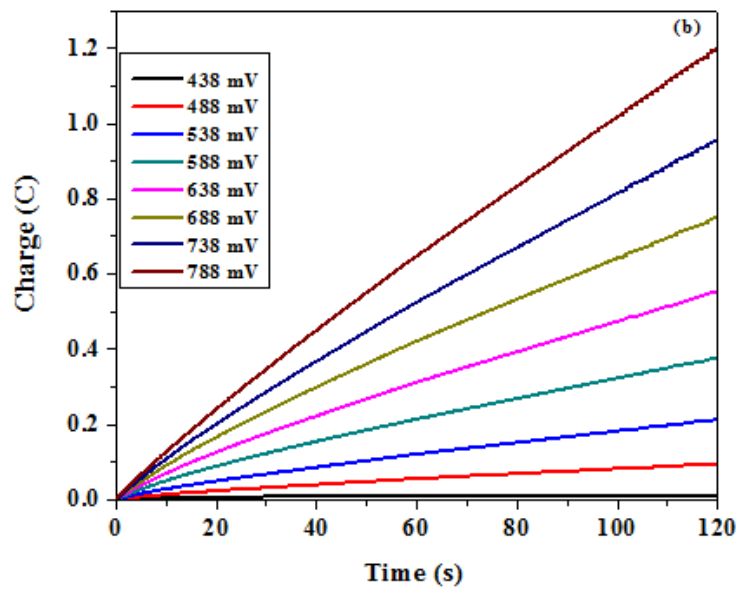
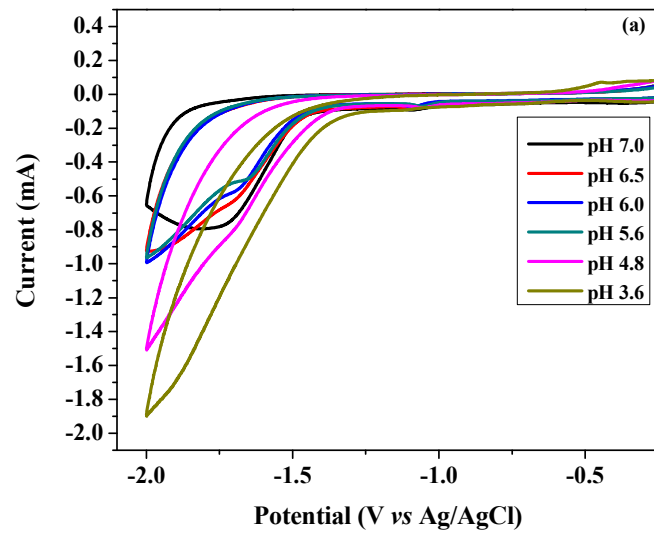


Fig. 1. Cyclic voltammograms of 0.25 M phosphate buffer solutions at pH 7.0 with and without complex **1** (0.1 mM). Conditions: GC working electrode (1 mm diameter), Pt wire counter electrode, Ag/AgCl reference electrode and 100 mV/s. The inset shows a magnified view of the Cu^{II}/Cu^I couple.



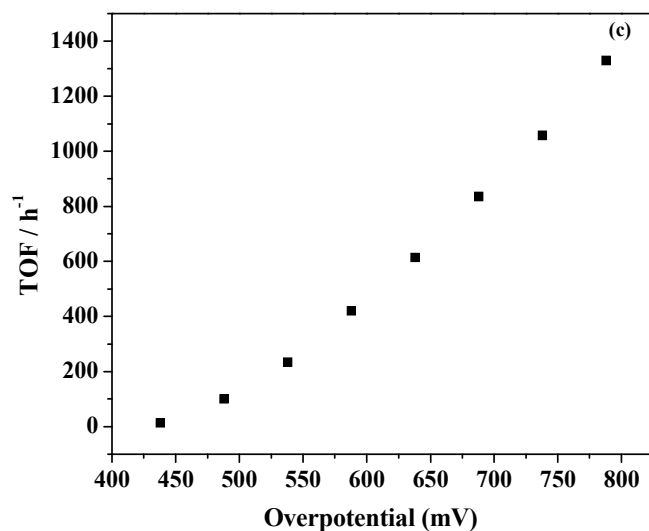


Fig. 2. (a) Cyclic voltammograms of complex **1** (0.10 mM) in 0.25 M buffer (pH 3.6, 4.8, 5.6, 6.0, 6.5, 7.0) at a glassy carbon electrode and a scan rate of 100 mV/s for water reduction. (b) Charge buildup of complex **1** (2.8 μ M) versus overpotentials (mV versus SHE) in 0.25 M phosphate buffer at pH 7.0. All data have been deducted blank. (c) Turnover frequency (mol H₂/mol catalysts/h) for electrocatalytic hydrogen production by complex **1** (2.8 μ M) under a series of overpotentials (mV versus SHE).

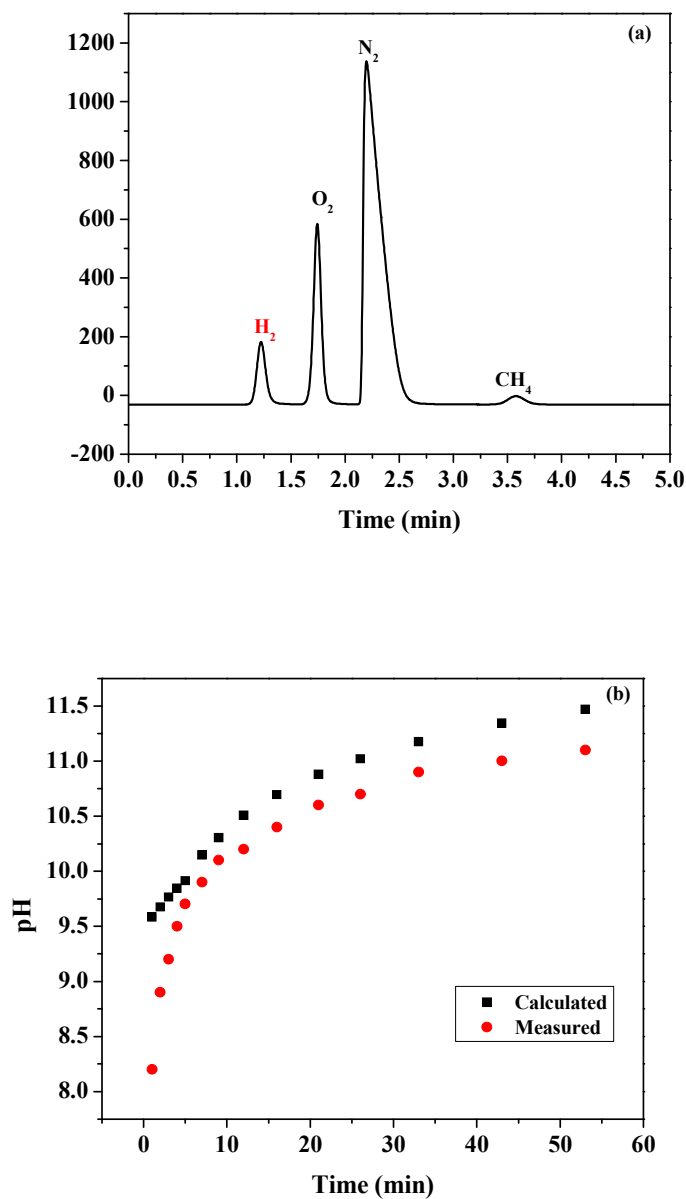
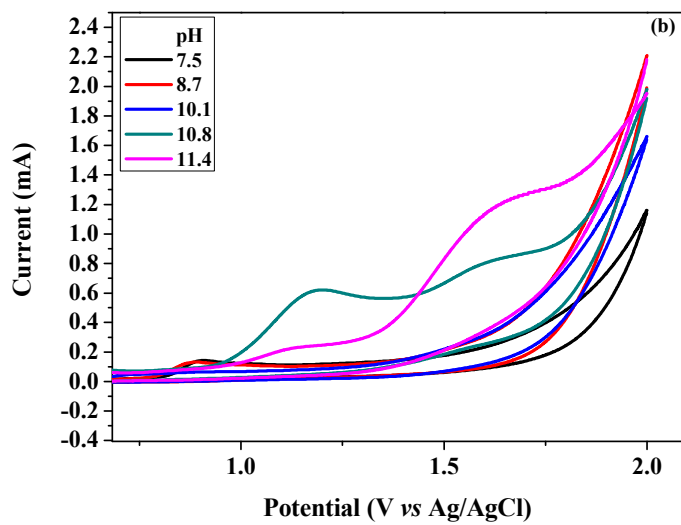
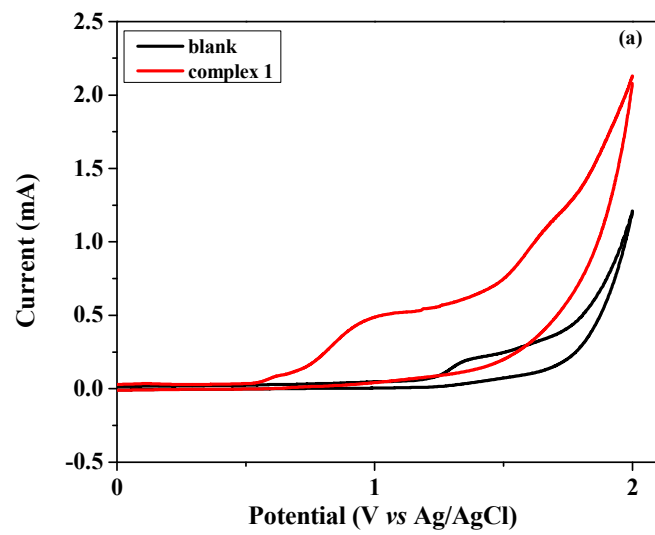


Fig. 3. (a) GC traces after a 1-h controlled-potential electrolysis at -1.20 V SHE of $2.2 \mu\text{M}$ complex **1** in 0.25 M phosphate buffer, pH 7.0. A standard of CH_4 was added for calibration purposes. (b) Measured (black) and calculated (red) pH changes assuming a 96.5% Faradic efficiency of complex **1** during electrolysis. (the theoretical

pH change over time can be calculated by the equation of $\text{pH} = 14 + \lg \frac{\sum It}{FV}$ where I = current (A), t = time (s), F = Faraday constant (96485 C/mol), V = solution volume (0.05 L)).



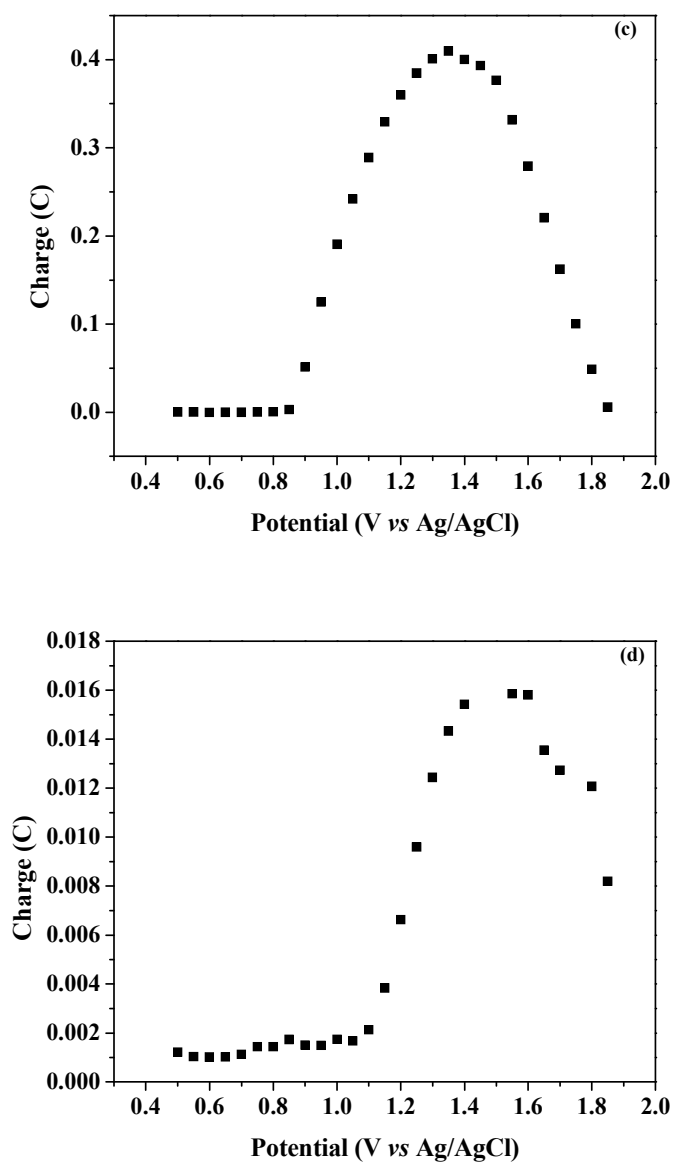


Fig. 4. (a) Cyclic voltammograms of the buffer with (red line) and without (black line) complex **1**. (b) Cyclic voltammograms of complex **1** (0.1 mM) in 0.25 M buffer (pH 7.5-11.4). (c) Charge buildup of complex **1** (0.1 mM) versus applied potentials (pH 10.8). (d) Charge buildup of complex **1** (0.1 mM) versus applied potentials (pH 8.7). Conditions: Pt counter electrode, Ag/AgCl reference electrode, scan rate 100 mV/s, 2 min. All data have been deducted blank.

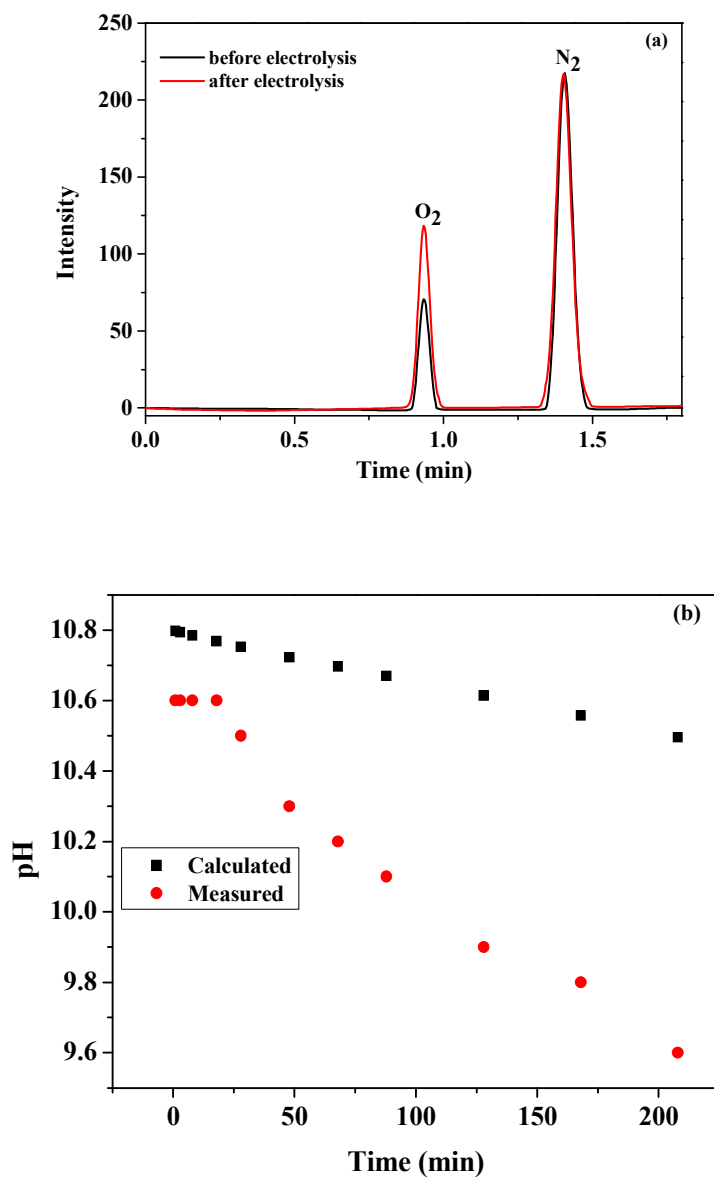


Fig. 5. (a) Normalized gas chromatographic trace before (black line) and after (red line) electrolysis in the presence of complex **1** for 5 h. 0.25 M phosphate buffer, pH 10.8, 2.8 μM complex **1**, ITO working electrode (1.32 cm^2), Pt counter electrode, Ag/AgCl reference electrode, applied potential 1.20 V vs Ag/AgCl. (b) Measured (red) and calculated (black) pH changes assuming a 100% Faradaic efficiency of complex **1** during the electrolysis.